Characterisation of the Processing Behaviour of Unidirectional Continuous Fibre Reinforced Thermoplastic Sheets

G.B. McGuinness, C.M. Ó Brádaigh
Composites Research Unit,
University College, Galway, Ireland.

(Presented at the Fourth International Conference on Flow Processes in Composite Materials, FPCM '96, University of Wales, Aberystwyth, September 1996)

Abstract

The in-plane shearing behaviour of laminates of unidirectional carbon fibre reinforced PEEK over a range of processing temperatures is studied. Shearing deformation is imposed on laminates via a four bar linkage (known as the picture-frame apparatus) which is loaded by a test machine. Force versus displacement data is presented for experiments conducted at different rates and temperatures, and the results are interpreted in terms of continuum mechanics models which treat the composite as an anisotropic fluid constrained to be inextensible in the reinforcement direction. The results of the study are compared to published data from experiments involving torsional rheometry with this material, and are found to be in disagreement. A discussion of the possible reasons for this is provided, and it is concluded that picture-frame shear testing is a more appropriate characterisation test than torsional rheometry. The picture-frame experiment results are also compared to reported squeeze flow characterisations of the transverse flow properties of the material, and are found to agree reasonably well. Material parameters which, together with the rheological models developed, describe the in-plane forming behaviour of carbon fibre reinforced PEEK are presented.

1 Introduction

Sheet-forming with composite materials

Sheet-forming technologies are currently being developed for continuous fibre reinforced thermoplastic and thermoset materials [1, 2]. These processes rely almost completely on the ability of the material systems to shear along the fibre directions in order to take on shapes of double curvature without buckling or other damage. The in-plane shearing properties of unidirectionally reinforced polymeric composites under processing conditions must be well understood if

production techniques for sheet-formed composite structures are to be improved. The material used for this work is carbon fibre reinforced PEEK, an ICI product commercially known as APC-2 [3].

Process Models

Much recent work has focused on the development of mathematical models, which provide the fabricator with a greater understanding of the mechanics of forming [4]. The first step to understanding sheet-forming processes is to identify the basic physical mechanisms at work during forming. The dominant characteristic of this type of material in the molten state is the very high resistance to deformation in the fibre direction compared to other unreinforced directions. The fibre directions may be considered *inextensible* during flow, resulting in a material which deforms primarily in shear, along and transverse to the fibre direction. Shearing in the plane of the sheet is required if shapes of double curvature are to be formed, and this is achieved by sliding of the fibres relative to one another (Figure 1 (a)). In a unidirectional material there appears to be no limit to how much intraply shear can be accommodated. Interply shear (Figure 1 (b)) is the relative motion of individual plies during forming, and occurs when single or double curvature parts are formed from multi-ply laminates. This mechanism is facilitated by the presence of a resin rich layer between plies [5]. The third mechanism is resin percolation (Figure 1 (c)). Resin flow relative to the fibres is not as significant with high viscosity thermoplastic matrices as it is with thermoset composites, but is necessary for consolidation. Pressure gradients along the material during forming lead to a squeeze flow mechanism (Figure 1 (d)) which strongly influences part thickness.

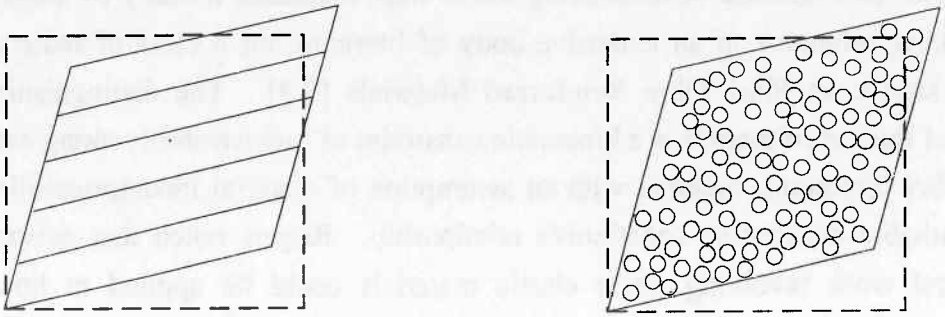

Longitudinal Shear Transverse Shear

(a) Intraply Shearing Mechanisms

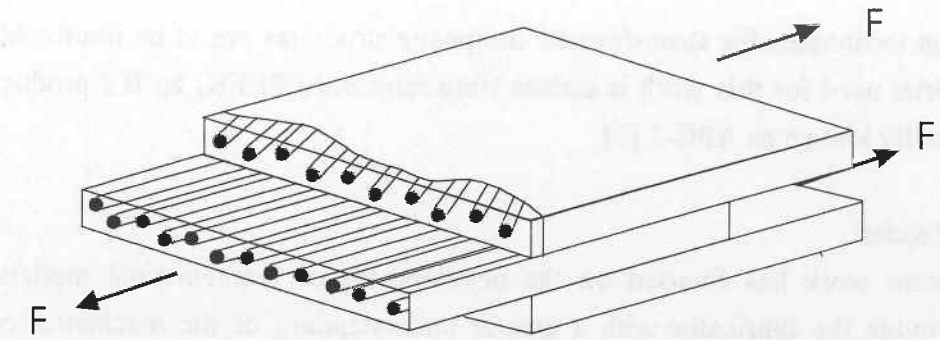

(b) Interply Slip Mechanism

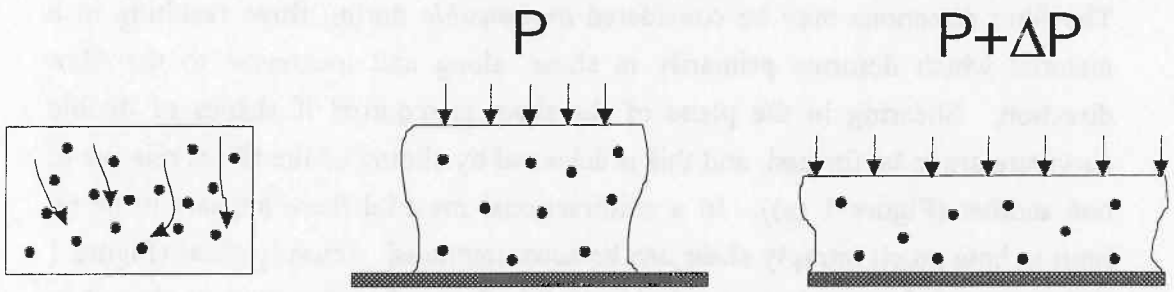

(c) Resin Percolation

(d) Squeeze Flow due to Pressure Gradient

Figure 1 Forming Mechanisms for Continuous Fibre Reinforced Thermoplastic Sheets

Rheological models for the forming behaviour of sheets of composite material with one or two families of reinforcing fibres were discussed initially by Rogers [6], making reference to an extensive body of literature on a class of material models known as Ideal Fibre Reinforced Materials [7,8]. The distinguishing feature of this set of models is a kinematic constraint of inextensibility along each set of fibre directions, together with an assumption of material incompressibility and a suitable anisotropic constitutive relationship. Rogers noted that existing theoretical work involving linear elastic materials could be applied to linear viscoelastic and viscous materials by invoking the viscoelastic correspondence principle, and presented possible approaches to rheological characterisation of composite materials [6].

Rheological Characterisation

The problem of characterising the intraply flows involved in forming a composite part with unidirectional plies of carbon fibre reinforced PEEK has previously been attempted using torsional rheometry and squeezing flow methods. The initial torsional rheometry work was carried out by Groves, who reports measurements made with a standard parallel plate torsional rheometer on samples of carbon and glass fibre reinforced Newtonian resin as shown in Figure 2 [9].

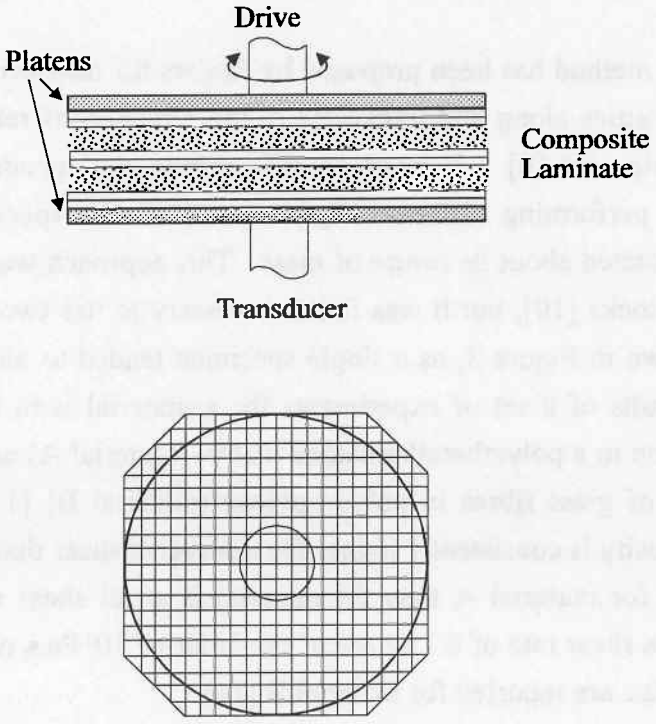

Figure 2 Torsional rheometer and "isotropic" test sample [9]

Small strain dynamic measurements were made using a sinusoidal input, and direct steady shear data was obtained using a triangular wave input. These experiments involve shear at all angles to the direction of reinforcement, which had the consequence that test results for 25 mm diameter cross ply and unidirectionally reinforced laminates are reported to be similar. The behaviour of the material in this test is referred to as the "isotropic" response of the material [9]. A linear viscoelastic model is used to interpret the results of the oscillatory tests with apparent Maxwell viscosities (defined in terms of the dynamic viscosity η' as $\eta_M = \eta'(1 + 1/\tan^2\delta)$) reported for different strains and strain rates. The effect of strain (or amplitude of oscillation) is noted to be minimal. Isotropic shearing viscosities are reported for the steady shear tests conducted at different strain

rates. For carbon fibre reinforced PEEK, the Maxwell and steady shear viscosities are reported to be of the order of 10^4 Pa.s.

The issue of whether the resin rich layers (which tend to form both between adjacent plies and also where the material is in contact with a tool) will have an effect on the shear flow distribution is examined in an indirect manner, but no physical evidence that the required shearing flows actually take place is presented [9].

A convenient method has been proposed by Rogers for measuring the anisotropic shearing viscosities along and transverse to the direction of reinforcement using the same equipment [6]. It involves off-centring the specimen to a specific position, and performing different experiments with the specimen in the same position but rotated about its centre of mass. This approach was implemented by Groves and Stocks [10], but it was found necessary to use two specimens in the positions shown in Figure 3, as a single specimen tended to move. Groves et al report the results of a set of experiments for a material with 60% carbon fibre volume fraction in a polyetheretherketone matrix (material A) and a material with 35% volume of glass fibres in polypropylene (material B) [11]. The apparent Maxwell viscosity is consistently higher for transverse shear than for longitudinal, and is higher for material A than for material B at all shear rates. Values for material A at a shear rate of 0.1 s^{-1} are of the order of 10^4 Pa.s while values of the order of 10^3 Pa.s are reported for material B [11].

Cogswell gives a review of efforts in the area of rheological characterisation of composite melts up to 1990, and compares the intraply viscosity results obtained by several researchers using the techniques described above [1]. Values for steady flow, complex and dynamic viscosities for both longitudinal and transverse shear are reported, varying between 3,200 Pa.s and 7,400 Pa.s. The longitudinal viscosity is higher by an average factor of 1.3. This is compared with viscosity values of neat PEEK in the region of 700 Pa.s.

A research programme to investigate the effect of fibre reinforcement on a Newtonian matrix fluid has been undertaken by Jones and co-workers [12, 13]. Specimens consisting of between 20% and 60% volume fraction nylon fibres and a Golden Syrup matrix were subjected to oscillatory shear, resulting in dynamic longitudinal and shear viscosities which are an order of magnitude larger than that of the neat syrup [13]. At volume fractions of 20% and 40%, the longitudinal value exceeds the transverse value, but at 60% volume fraction this is reversed.

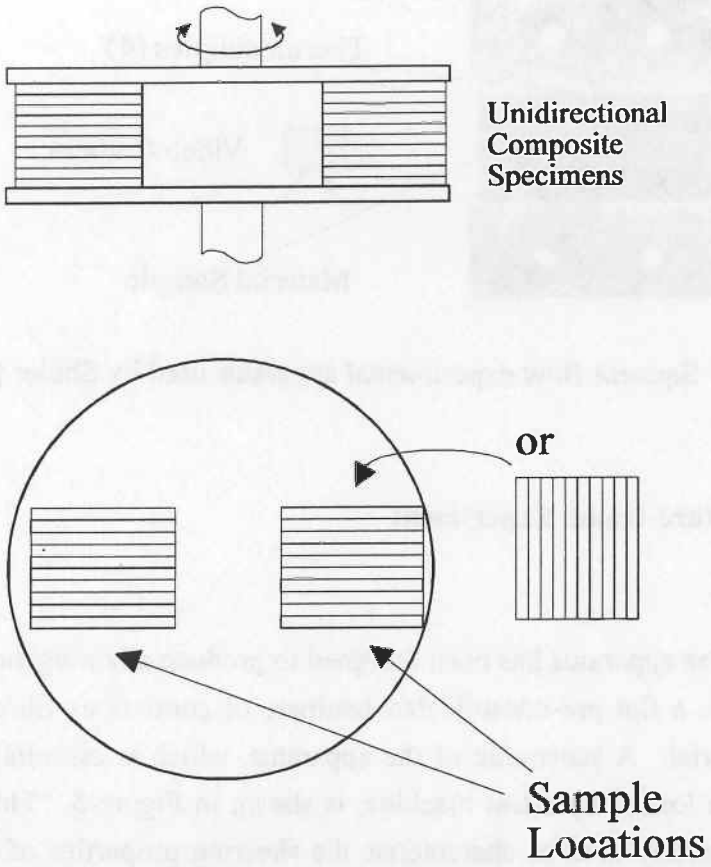

Figure 3 Off-axis geometry for anisotropic measurements [10].

Shuler investigates the rheological properties of aligned fibres embedded in a viscous fluid using a squeeze flow experiment [14]. Model material systems involving clay matrices reinforced by nylon and glass fibres were used to demonstrate the effect of the presence of fibres on the properties of the material during flow. Squeeze flow experiments with APC-2 (unidirectional carbon fibre reinforced PEEK), in which the flow conditions were directly observed and recorded on video, were modelled using a Carreau model, with a viscosity parameter of 2.5×10^6 Pa.s. at 370°C (Figure 4). Wang and Gutowski have also studied squeeze flow of APC-2, and characterise the response in terms of a power-law model [15].

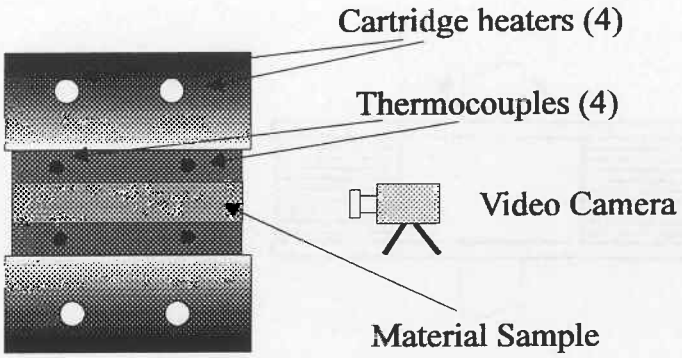

Figure 4 Squeeze flow experimental apparatus used by Shuler [15].

2 The Picture-frame Experiment

Description

The picture-frame apparatus has been designed to produce a homogenous in-plane shearing flow in a flat pre-consolidated laminate of continuous fibre reinforced composite material. A schematic of the apparatus, which is essentially a square four-bar linkage loaded by a test machine, is shown in Figure 5. This apparatus has been successfully used to characterise the shearing properties of glass fabric reinforced Nylon composite laminates at processing temperatures [16,17]. Experiments are performed within an environmental chamber, with force and displacement data acquisition to a personal computer. Characterisations are conducted at different temperatures within the materials processing window and over a range of constant actuator displacement rates consistent with the shear rates experienced in sheet-forming processes.

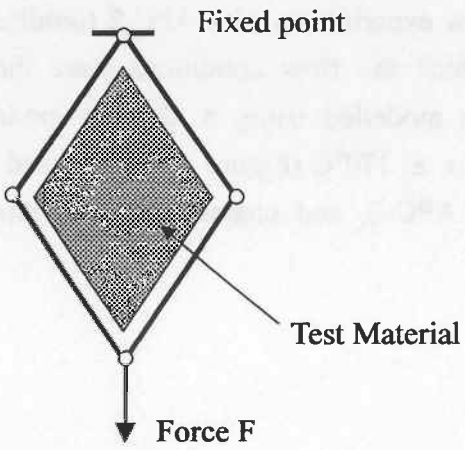

Figure 5 Schematic representation of the operation of the picture-frame apparatus.

Procedure

Specimens are cut from laminates of APC-2 which have been consolidated at a pressure of 0.4 MPa and a temperature of 380°C. The experimental approach to testing unidirectional materials is not straightforward since the attachment of specimens to the bars of the picture-frame apparatus presents a practical problem. Testing with fabric reinforced composite specimens has involved drilling holes in each specimen at the locations shown in Figure 6 and attaching it to the apparatus by means of appropriately located pins [16]. For unidirectional laminates, this method tends to cause a failure of the material at the attachment pins.

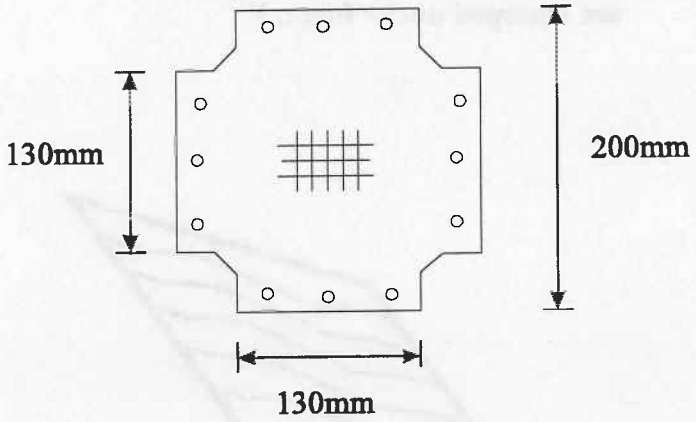

Figure 6 Shape of picture-frame apparatus composite specimen.

Efforts were initially concentrated on specimens which fit neatly inside the frame of the apparatus [*]. For this approach it is necessary that fibre ends are allowed to rotate at the point where they are in contact with the bars of the apparatus in order to ensure that the prescribed kinematics are, in fact, produced. If clamped, the fibres would either be forced to bend severely at the point of clamping, slip out of the clamping device or stretch to form an "S" shape during deformation (Figure 7).

Unidirectional laminates were successfully shear tested by enclosing an appropriately sized laminate in an envelope of polymeric diaphragm material (see Figures 8, 9 [18]). The envelope is clamped to the picture-frame apparatus but the composite, though pressed tightly against the bars, is not clamped. Throughout each experiment of this kind, the diaphragm envelope is held under vacuum which helps prevent deconsolidation.

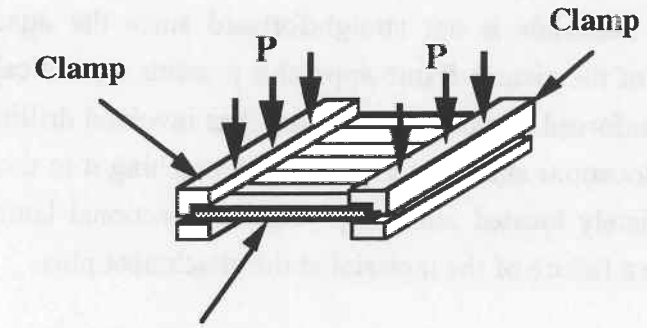

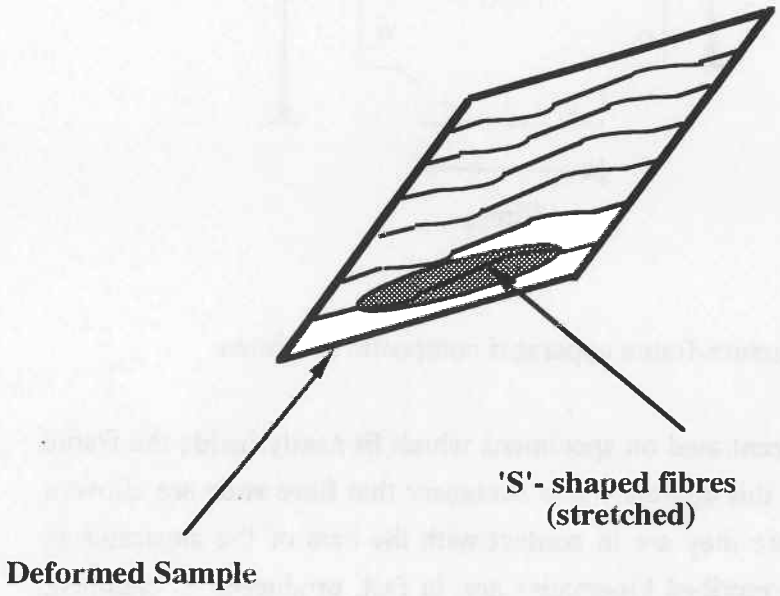

Figure7 Effect of clamping of fibres during picture-frame testing.

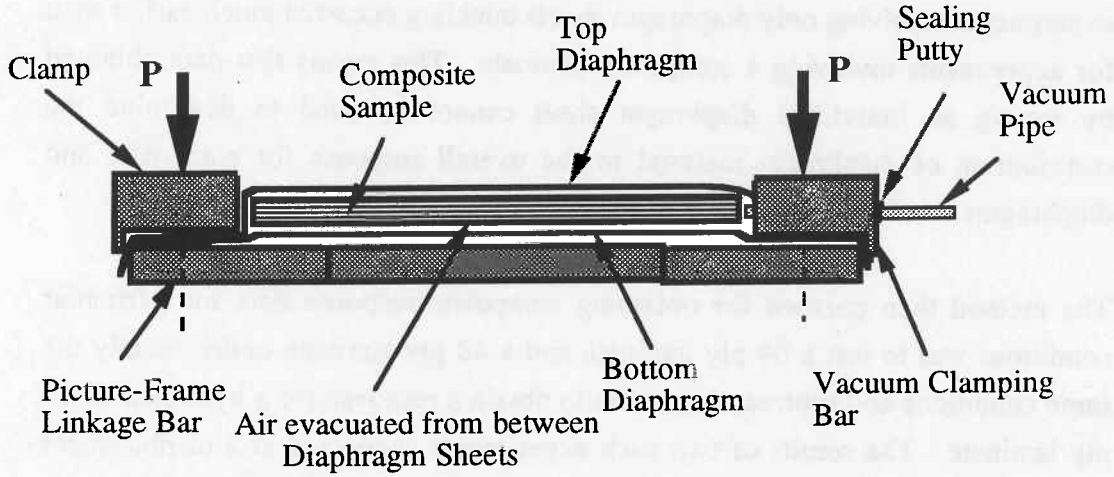

Figure 8 Detailed diagram of method of attachment of diaphragm and composite to the picture-frame apparatus for unidirectional material tests .

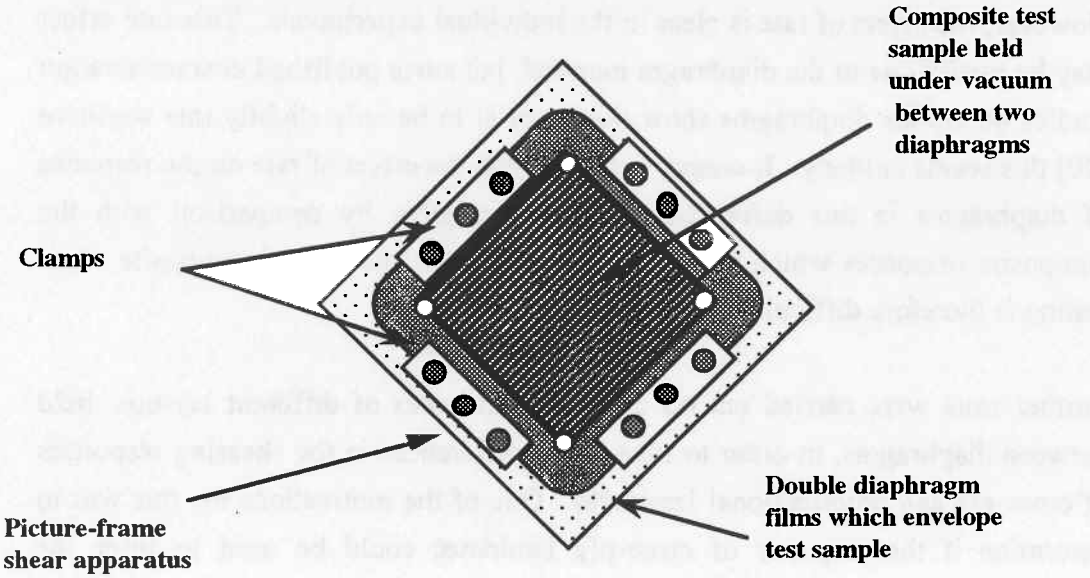

Figure 9 Picture-frame apparatus holding a unidirectional composite specimen between diaphragms.

Although successful, this approach to shear testing presents additional problems. It is necessary to quantify the contribution of the diaphragm material to the overall force response so that it can be subtracted out to give reliable data for the composite alone. The diaphragm material used was Upilex R [19]. In experiments involving only diaphragm sheets buckling occurred much earlier than for experiments involving a composite laminate. This means that data obtained by testing an individual diaphragm sheet cannot be used to determine the contribution of diaphragm material to the overall response for composite and diaphragms.

The method then pursued for obtaining composite response data for particular conditions was to test a 64 ply laminate and a 48 ply laminate under exactly the same conditions and subtract the results to obtain a response for a hypothetical 16 ply laminate. The results of two such experiments conducted at a displacement rate of 100 mm/min are shown in Figure 10, together with the inferred response for 16 plies of material. The same set of experiments has been carried out at 10 mm/min. The subtracted responses for 16 plies of APC-2 at 10 mm/min and 100 mm/min are shown in Figure 11. The subtracted load responses are practically identical which suggests that the response of APC-2 is not rate dependent. However, the effect of rate is clear in the individual experiments. This rate effect may be totally due to the diaphragm material, but since published characterisation studies on Upilex diaphragms show the material to be only slightly rate sensitive [20] this seems unlikely. It seems, however, that the effect of rate on the response of diaphragms in this deformation is non-negligible by comparison with the composite responses which must be measured. This method of composite shear testing is therefore difficult to interpret.

Further tests were carried out on cross-ply laminates of different lay-ups, held between diaphragms, in order to investigate differences in the shearing responses of cross-ply and unidirectional laminates. One of the motivations for this was to determine if the response of cross-ply laminates could be used to infer the properties of unidirectional material, since cross-ply laminates may be tested in a more straightforward manner by attaching an over-sized specimen to the faces of the bars via pins. Two different lay-ups were used to investigate this possibility. Experiments were conducted at 10 mm/min and 100 mm/min for laminates of $[0°_{12}/90°_{12}]_S$ and for 48 ply symmetric laminates of completely interspersed 0° and 90° plies $[(0°/90°)_{12}]_S$. Upilex diaphragms were again used to contain the material during testing. The results of these experiments are shown in Figure 12, where it

is emphasised that these results include the effect of diaphragms. The responses of the macro $[0°_{12}/90°_{12}]_S$ and fully interspersed $[(0°/90°)_{12}]_S$ cross-ply laminates are very close over the whole range of deformation for both rates. However, the force response for unidirectional laminates is not as high as for the cross-ply laminates at either displacement rate. After 25 mm of deformation, the cross-ply force levels are approximately 25% higher than the corresponding unidirectional experiments, which introduces doubt as to how accurately the shearing properties of unidirectional laminates can be inferred from cross-ply experiments.

Nonetheless, cross-ply experiments which do not involve diaphragms are of interest, since (i) these tests provide the most direct measurement of composite response of any of the tests attempted or reviewed and (ii) many structures are formed using cross-ply or quasi-isotropic lay-ups. The cross-ply test specimens are cut into the shape shown in Figure 6 from 32 ply $[0_4/90_4/]_{2s}$. laminates. Following unsatisfactory experiments, it was decided to fit steel bushings to prevent specimen failure at the pin location holes. The results of experiments conducted at rates of 10 mm/min, 100 mm/min, 300 mm/min and 500 mm/min at a temperature of 360°C are shown in Figure 13. The expected rate dependency of the material is confirmed, with the force response for the faster rates reaching 225 Newtons after 20 mm of displacement. These experiments were repeated at 370°C and a rate dependent response was again observed (Figure 14), with peak loads for the 500 mm/min case of 140 Newtons. Results for experiments conducted at 380°C are shown in Figure 15. For this temperature, there is a substantial difference between the loads recorded for the 300 mm/min and 500 mm/min cases. For a 500 mm/min actuator displacement rate at 380°C, the load levels again reach values of 225 Newtons after 20 mm of displacement, but the responses for the slower rates do not exceed 80 Newtons.

The results of experiments carried out at 100 mm/min at temperatures of 350°C, 360°C, 370°Cand 380°C are compared in Figure 16. The temperature dependence of the mechanical response of APC-2 during processing is clearly seen.

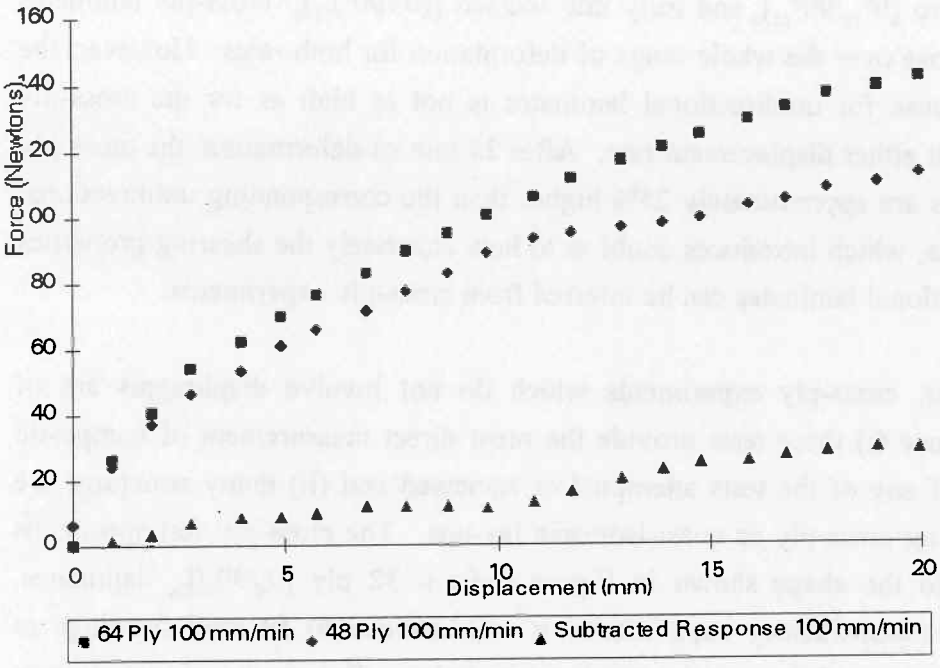

Figure 10 Force versus displacement for 64 ply laminate with diaphragms, 48 ply laminate with diaphragms and inferred response for a 16 ply composite specimen.

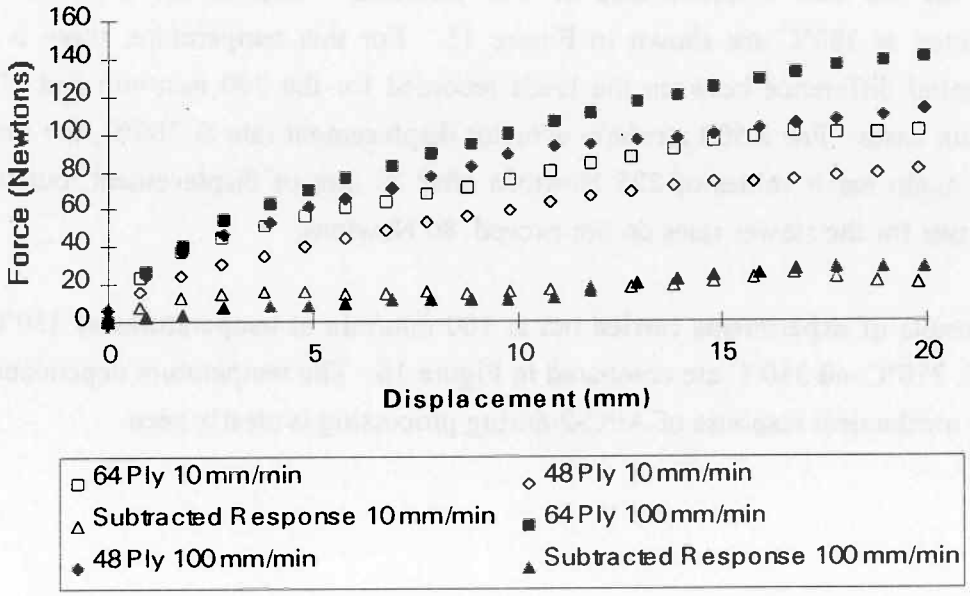

Figure 11 Response of 16 ply laminate of APC-2 estimated by subtraction of results for 48 ply laminate with diaphragms from 64 ply laminate with diaphragms. Results for 100 mm/min and 10 mm/min.

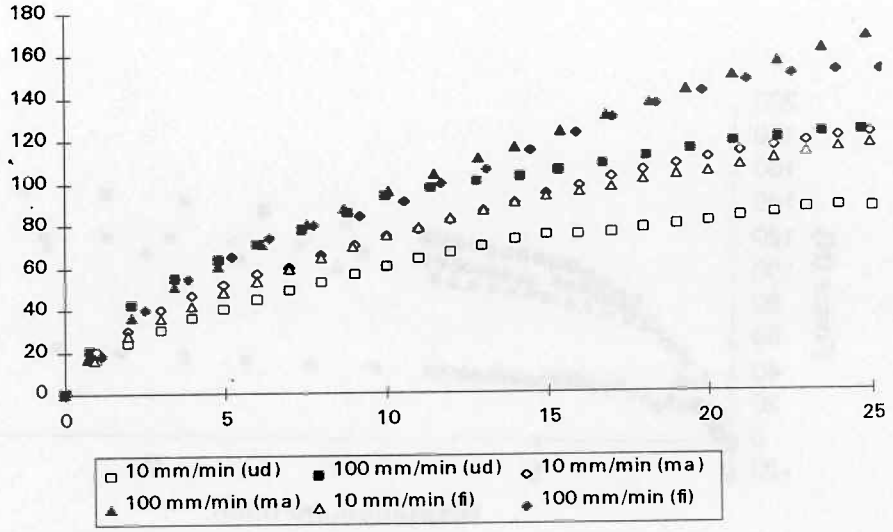

Figure 12 Comparison of picture-frame shearing responses of 48 ply laminates of APC-2 with different lay-ups held between Upilex R diaphragms.

(ud) : Unidirectional lay-up

(ma) : Macro cross-ply. $(0°_{12}/90°_{12})_S$

(fi) : Fully interspersed. Symmetric cross-ply with adjacent plies at 90 degrees to each other.

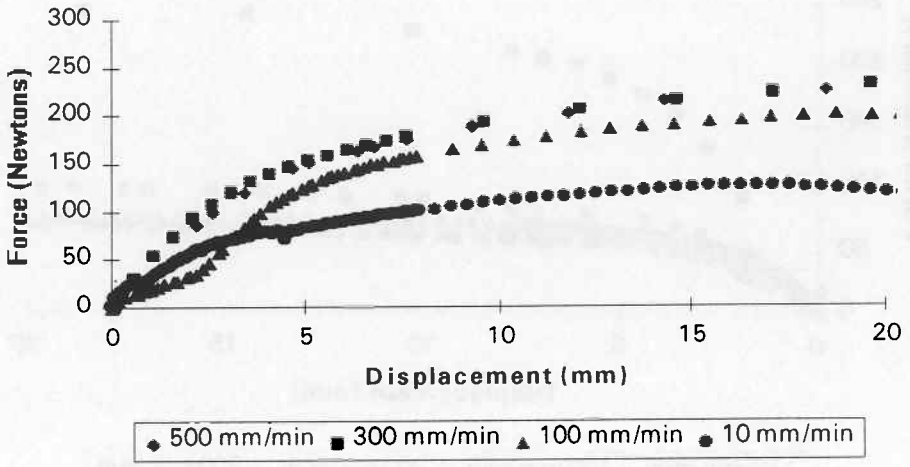

Figure 13 Force response of APC-2 specimens as per Figure 6 at 360°C.

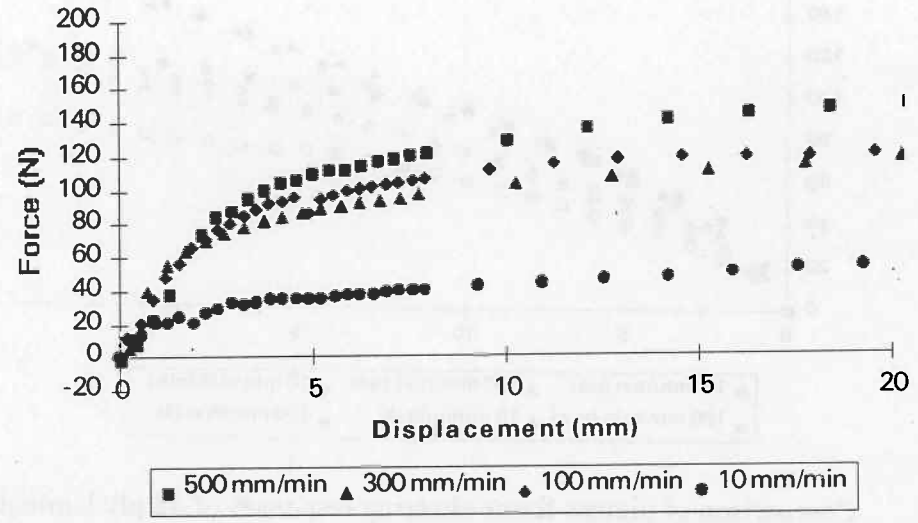

Figure 14 Force response of APC-2 specimens as per Figure 6 at 370°C.

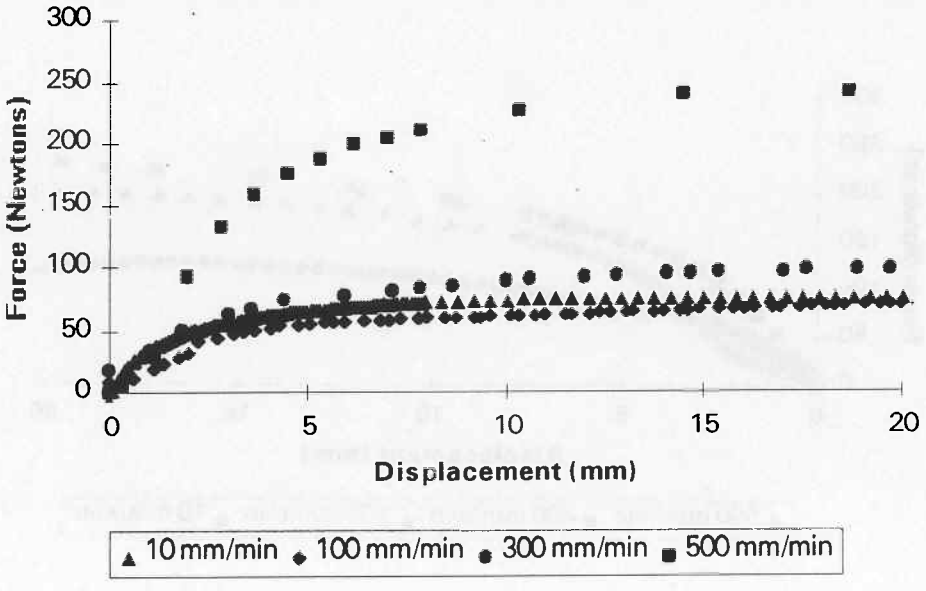

Figure 15 Force response of APC-2 specimens as per Figure 6 at 380°C.

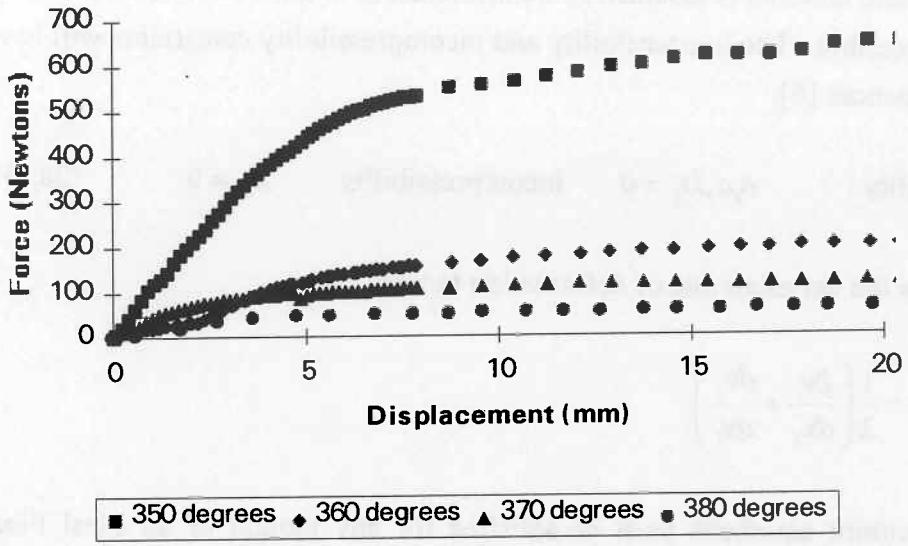

Figure 16 Effect of temperature on force response of APC-2
(displacement rate = 100 mm/min, specimens as per Figure 6)

3 Rheological Models

The concept of the *Ideal Fibre Reinforced Material*, is used to develop material models capable of describing the behaviour exhibited by APC-2 in the experiments reported in Section 2. This body of theory is described in detail by Spencer [7, 8] and was first used to describe composites forming behaviour by Rogers[6]. The reinforced molten polymer material is idealised as a viscous material subject to the kinematic constraints of incompressibility and inextensibility in the fibre direction. A form of this material model which is capable of describing large strains and strain rates, commonly encountered in forming situations, and which features material anisotropy is presented.

Assumptions

In the theory of Ideal Fibre Reinforced Materials, the assumption is made that the fibres are convected with the deforming material. If the initial local fibre direction is given by the unit vector **A** and the current fibre direction is denoted **a**, then fibre orientations may be updated as follows :

$$a_i = \frac{\partial x_i}{\partial X_j} A_j \qquad (1)$$

The composite material is assumed to be inextensible in the fibre direction and to be incompressible. The inextensibility and incompressibility constraints will have the consequences [6]:

Inextensibility : $a_i a_j D_{ij} = 0$ Incompressibility : $D_{ii} = 0$ (2a,b)

where D_{ij} is the cartesian rate of deformation tensor :

$$D_{ij} = \frac{1}{2}\left(\frac{\partial v_i}{dx_j} + \frac{dv_j}{dx_i} \right)$$

These constraint equations must be satisfied for any motion of an Ideal Fibre Reinforced Fluid.

Stress

As a consequence of the kinematic constraints employed in the model, the Cauchy stress tensor may be decomposed as follows [7, 8] :

$$\sigma_{ij} = \tau_{ij} - p\delta_{ij} + Ta_i a_j \qquad (3)$$

p is an arbitrary hydrostatic pressure due to the incompressibility contraint and T is an arbitrary fibre tension stress associated with the inextensibility constraint. τ_{ij} is known as the extra stress and depends on the kinematic history of the material element.

Constitutive Models

The approach taken by Duffy to the flow of an anisotropic viscous fluid involves the use of embedded co-ordinate systems which are convected with the deforming material. This approach results in curvilinear co-ordinate systems which are non-orthogonal. For convenience, the relationships determined using this approach will then be transformed to the familiar spatial cartesian system x_i, which is taken to be initially co-incident with the material co-ordinate system X_r.

Duffy relates the convected covariant stress tensor $\tau_{ij}^{\cdot}$ to the convected covariant rate of strain tensor, which will be denoted d_{ij}, by means of a scalar quantity and a physical constant tensor [21]. The concept of a physical constant tensor quantity was introduced by Oldroyd as a tensor whose components are equal in any convected co-ordinate system. Therefore, both the scalar quantity and the

components of the physical constant tensor remain constant as the deformation develops. For the most general anisotropic linearly viscous material τ_{ij} can be related to d_{ij} by means of a physical constant tensor C_{ij}^{lk}, with possible scalar quantities absorbed into its components [21].

$$\tau_{ij} = C_{ij}^{lk} d_{lk} \tag{4}$$

A physical constant tensor following Oldroyds definition satisfies the requirement :

$$\frac{d}{dt} C_{ij}^{lk} = 0 \tag{5}$$

If the material model is to describe the two shearing modes identified in Section *.*, the longitudinal and transverse viscosity parameters η_L and η_T must be included in the material description. If the material axes X_1 coincides with the reinforcement direction, the appropriate non-zero components of the viscosity tensor C_{ij}^{lk} will be :

$$C_{11}^{11} = 4\eta_L - 2\eta_T \qquad C_{23}^{23} = C_{32}^{32} = C_{23}^{32} = C_{32}^{23} = \eta_T \tag{6}$$

$$C_{22}^{22} = C_{33}^{33} = 2\eta_T \qquad C_{12}^{12} = C_{21}^{21} = C_{12}^{21} = C_{21}^{12} = \eta_L$$

$$C_{13}^{13} = C_{31}^{31} = C_{13}^{31} = C_{31}^{13} = \eta_L$$

It can be necessary to allow the viscosity parameters to be shear-rate dependent and this is achieved, in this case, by introducing the power-law relationship :

$$\eta_L = m_L \left(\sqrt{2 d_{ij} d_{ij}} \right)^{n-1} \qquad \eta_T = m_T \left(\sqrt{2 d_{ij} d_{ij}} \right)^{n-1} \tag{7a,b}$$

Note that there are a number of other invariant quantities associated with the tensor quantities D_{ij} and $a_i a_j$ which could also be used to describe the dependence of the viscous parameters on the flow variables.

Transformation to Fixed Spatial Co-ordinate System

The transformation of the constitutive equations to a fixed spatial co-ordinate system is achieved in the following way:

$$B_{ij}^{kl} = \frac{\partial X^p}{\partial x^i}\frac{\partial X^q}{\partial x^j}\frac{\partial x^k}{\partial X^m}\frac{\partial x^l}{\partial X^n}C_{pq}^{mn} \tag{8}$$

Note that the tensor components B_{ij}^{kl} (which can now be written B_{ijkl} for Cartesian co-ordinates) can become substantially different to the C_{ij}^{lk} as the deformation becomes large. The general form of the constitutive relationship for an anisotropic viscous material which undergoes large deformations is therefore (in Cartesian spatial co-ordinates):

$$\sigma_{ij} = B_{ijkl}D_{kl} - p\delta_{ij} + Ta_i a_j \tag{9}$$

where $B_{ijkl} = F_{km}F_{ln}C_{pq}^{mn}F_{ip}^{-1}F_{jq}^{-1}$ and F_{ij} are the components of the deformation gradient tensor.

4 Interpretation of the Picture-frame Experiment

Geometry of the picture-frame experiment

The geometry of a test specimen for use in the picture frame apparatus is shown in Figure 17. The length L of each side of the square piece is 200 mm, while the thickness t will be different for different test materials and lay-ups. The length of each bar in the picture frame apparatus is denoted L_{BAR}, and is 150 mm.

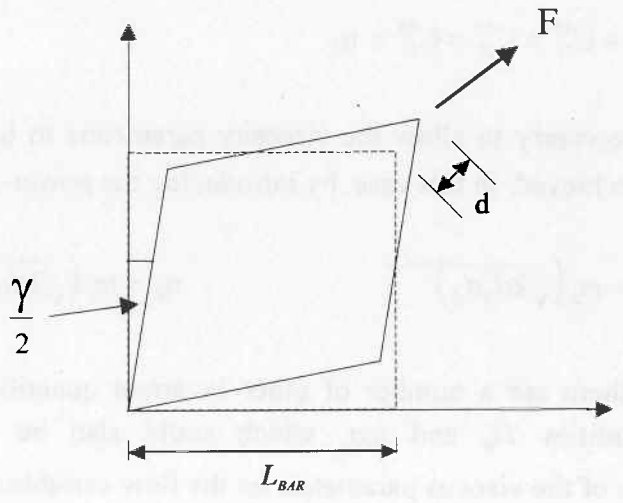

Figure 17 Geometry of the picture-frame experiment

The expression relating the displacement of the actuator to the angle γ is :

$$d = (2L_{BAR})\cos\left(\frac{\pi}{4} - \frac{\gamma}{2}\right) - \sqrt{2}L_{BAR} \tag{10}$$

and the expression relating the rate of displacement $\dot{d}$ with the shear rate $\dot{\gamma}$ is :

$$\dot{d} = L_{BAR}\dot{\gamma}\sin\left(\frac{\pi}{4} - \frac{\gamma}{2}\right) \tag{11}$$

In the experiment, a constant displacement rate is used, resulting in a varying shear rate $\dot{\gamma}$.

Kinematics

The kinematic conditions experienced by the material are uniform throughout the sheet. The picture frame kinematics are described in terms of the angle γ as :

$$F_{ij} = \begin{bmatrix} \cos\left(\frac{\gamma}{2}\right) & \sin\left(\frac{\gamma}{2}\right) & 0 \\ \sin\left(\frac{\gamma}{2}\right) & \cos\left(\frac{\gamma}{2}\right) & 0 \\ 0 & 0 & \frac{1}{\cos\gamma} \end{bmatrix} \quad D_{ij} = \begin{bmatrix} -\frac{1}{2}\dot{\gamma}\frac{\sin\gamma}{\cos\gamma} & \frac{1}{2}\dot{\gamma}\frac{1}{\cos\gamma} & 0 \\ \frac{1}{2}\dot{\gamma}\frac{1}{\cos\gamma} & -\frac{1}{2}\dot{\gamma}\frac{\sin\gamma}{\cos\gamma} & 0 \\ 0 & 0 & \dot{\gamma}\frac{\sin\gamma}{\cos\gamma} \end{bmatrix} \tag{12}$$

It should be noted that the kinematic conditions of inextensibility and material incompressibility are satisfied.

Stress Response of Ideal Fibre Reinforced Viscous Fluid

The stress response of an Ideal Fibre Reinforced Viscous Fluid to the picture-frame conditions are :

$$\sigma_{11} = -\eta_L\dot{\gamma}\tan\gamma - p + T(x_1, x_2)\cos^2\frac{\gamma}{2} \tag{13a}$$

$$\sigma_{22} = -\eta_L\dot{\gamma}\tan\gamma - p + T(x_1, x_2)\sin^2\frac{\gamma}{2} \tag{13b}$$

$$\sigma_{33} = 2\eta_T\dot{\gamma}\tan\gamma - p \tag{13c}$$

$$\sigma_{12} = \eta_L\dot{\gamma}\frac{1}{\cos\gamma} + T(x_1, x_2)\sin\frac{\gamma}{2}\cos\frac{\gamma}{2} \tag{13d}$$

Equilibrium Equations

If body forces and inertial effects are neglected, the equilibrium equations are :

$$\sigma_{ij,j} = 0 \tag{14}$$

The extra stress distribution is uniform throughout the sheet since the kinematic conditions are uniform, but it is possible that the reaction stresses p and T vary spatially. The stress solution must satisfy :

$$\frac{\partial}{\partial x_j}\left(-p\delta_{ij} + Ta_i a_j\right) = 0 \tag{15}$$

Further information on the stress solution requires the specification of boundary conditions for both arbitrary stress quantities. It will be shown, however, that the arbitrary stress distributions are not required to determine the force response of the apparatus so the boundary conditions for these stresses are not needed in this analysis.

Interpretation

The interpretation of the results of experiments such as those reported here has been discussed in an earlier publication [22]. In summary, the force versus displacement response is determined using the principle of virtual power to equate the stress power induced in the material to the rate of work of the forces acting on the picture-frame apparatus :

$$F\dot{d} = \int_{\Omega} \sigma_{ij} D_{ij} d\Omega \tag{16}$$

Since the arbitrary tension and pressure stresses enter this expression as $Ta_i a_j D_{ij}$ and $p\delta_{ij} d_{ij} = pd_{ii}$, they make no contribution for flows which satisfy the kinematic constraints. Because the extra stresses are uniform throughout the sheet, the force versus displacement responses are given by :

$$F\dot{d} = L^2 t\left(\sigma_{ij} D_{ij}\right) \tag{17}$$

The stress response of a viscous material with distinct longitudinal and transverse shearing properties is :

$$F\dot{d} = L^2 t\left(\dot{\gamma}^2\left(\eta_L\left(\frac{1+\sin^2\gamma}{\cos^2\gamma}\right) + 2\eta_T\left(\frac{\sin^2\gamma}{\cos^2\gamma}\right)\right)\right) \tag{18}$$

If the power-law shear rate dependency of (7) is employed, then :

$$\left(\frac{F\dot{d}}{\dot{\gamma}^2 L^2 t}\frac{\cos^2\gamma}{(1+\sin^2\gamma)}\right)=\left(\dot{\gamma}\sqrt{\frac{1+3\sin^2\gamma}{\cos^2\gamma}}\right)^{n-1}\left(\left(m_L+m_T\left(\frac{2\sin^2\gamma}{1+\sin^2\gamma}\right)\right)\right) \quad (19)$$

which may be rewritten in the form :

$$\left(\frac{F\dot{d}}{\dot{\gamma}^2 L^2 t}\frac{\cos^2\gamma}{(1+\sin^2\gamma)}\right)\left(\sqrt{\frac{1+3\sin^2\gamma}{\cos^2\gamma}}\right)^{1-n}=\left(\left(m_L+m_T\left(\frac{2\sin^2\gamma}{1+\sin^2\gamma}\right)\right)\right) \quad (20)$$

This may be interpreted as shown in Figure 18, where a value of n must be chosen for which all experimental data falls on the straight line.

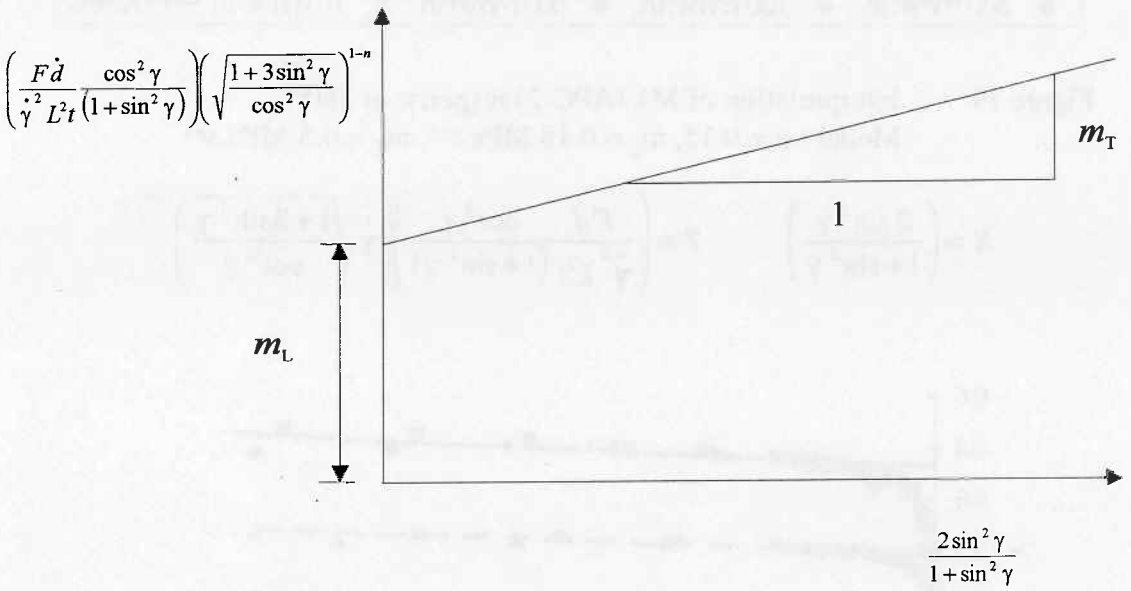

Figure 18 Interpretation of the picture-frame experiment in terms of an anisotropic power-law viscous model.

Interpretation of experiments

The graphical interpretation of the experimental results discussed in Section 2 for 360°C, 370°C and 380°C are now presented. A power law viscous model is seen to give a good representation of the behaviour of APC-2 at 360°C (Figure 19), but such good agreement is not found for the experiments conducted at 370°C and 380°C (Figures 20 and 21). In these cases, the material appears to exhibit a shear rate dependency which is more complex than can be described by a simple power law type model. Nevertheless, viscosity values or ranges for particular shear-rate

ranges can be obtained by using the appropriate one of the two power law models shown in the interpretation graphs.

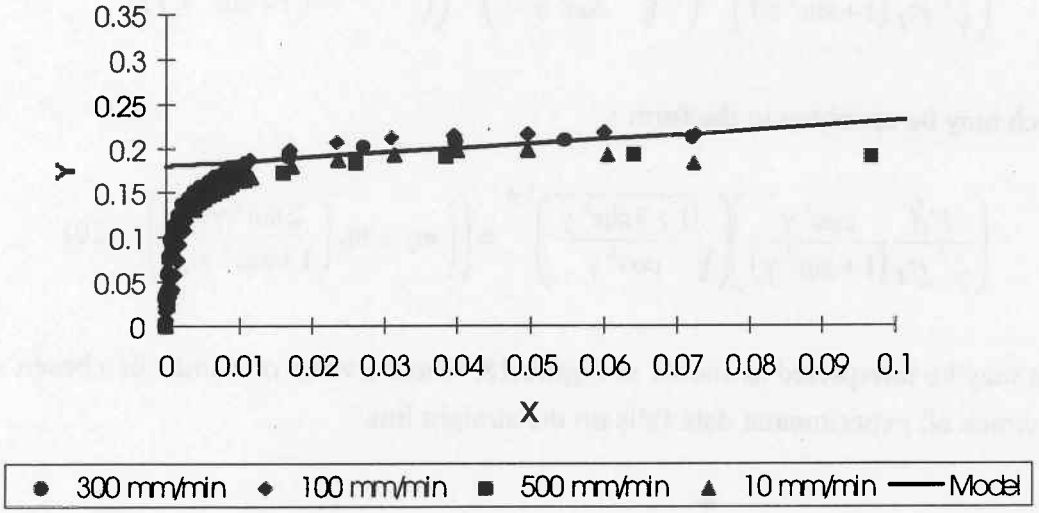

Figure 19 Interpretation of M1 (APC-2) response at 360°C.
Model : n = 0.15, m_L = 0.18 MPa.s^{n-1}, m_T = 0.5 MPa.s^{n-1}

$$X = \left(\frac{2\sin^2\gamma}{1+\sin^2\gamma} \right) \qquad Y = \left(\frac{F\dot{d}}{\dot{\gamma}^2 L^2 t} \frac{\cos^2\gamma}{(1+\sin^2\gamma)} \right) \left(\dot{\gamma} \sqrt{\frac{1+3\sin^2\gamma}{\cos^2\gamma}} \right)^{1-n}$$

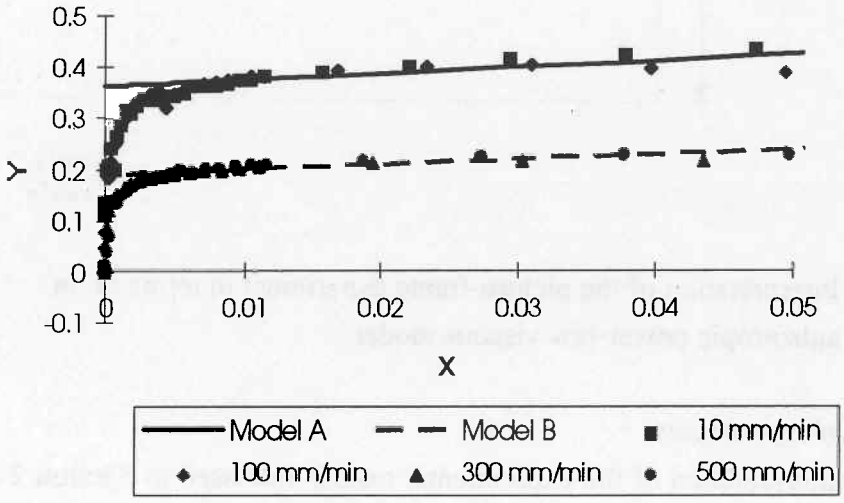

Figure 20 Interpretation of APC-2 response at 370°C.
Model A : n = 0.42, m_L = 0.36 MPa.s^{n-1}, m_T = 1.25 MPa.s^{n-1}
Model B : n = 0.4, m_L = 0.19 MPa.s^{n-1}, m_T = 1.0 MPa.s^{n-1}

$$X = \left(\frac{2\sin^2\gamma}{1+\sin^2\gamma} \right) \qquad Y = \left(\frac{F\dot{d}}{\dot{\gamma}^2 L^2 t} \frac{\cos^2\gamma}{(1+\sin^2\gamma)} \right) \left(\dot{\gamma} \sqrt{\frac{1+3\sin^2\gamma}{\cos^2\gamma}} \right)^{1-n}$$

$$X = \left(\frac{2\sin^2\gamma}{1+\sin^2\gamma} \right) \qquad Y = \left(\frac{F\dot{d}}{\dot{\gamma}^2 L^2 t} \frac{\cos^2\gamma}{(1+\sin^2\gamma)} \right) \left(\dot{\gamma} \sqrt{\frac{1+3\sin^2\gamma}{\cos^2\gamma}} \right)^{1-n}$$

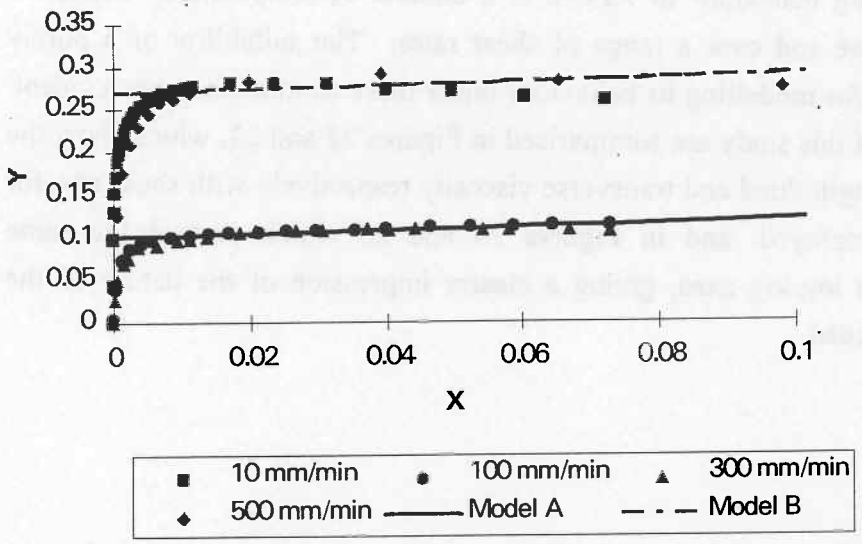

Figure 21 Interpretation of APC-2 response at 380°C.
Model A : n = 0.28, m_L = 0.1 MPa.s^{n-1}, m_T = 0.18 MPa.s^{n-1}
Model B : n = 0.28, m_L = 0.27 MPa.s^{n-1}, m_T = 0.18 MPa.s^{n-1}

$$X = \left(\frac{2\sin^2\gamma}{1+\sin^2\gamma} \right) \qquad Y = \left(\frac{F\dot{d}}{\dot{\gamma}^2 L^2 t} \frac{\cos^2\gamma}{(1+\sin^2\gamma)} \right) \left(\dot{\gamma} \sqrt{\frac{1+3\sin^2\gamma}{\cos^2\gamma}} \right)^{1-n}$$

	n	m_L (MPa.s^n)	m_T (MPa.s^n)
APC-2 (a), 380°C	0.28	0.27	0.18
APC-2 (b), 380°C	0.28	0.1	0.18
APC-2 (a), 370°C	0.42	0.36	1.25
APC-2 (b), 370°C	0.4	0.19	1.0
APC-2, 360°C	0.15	0.18	0.5

Table 1 Anisotropic viscous model parameters for APC-2.
APC-2 (a) 380°C Interpretation of results for 100 mm/min and 300 mm/min.
APC-2 (b) 380°C Interpretation of results for 500 mm/min and 10 mm/min.
APC-2 (a) 370°C Interpretation of results for 10 mm/min and 100 mm/min.
APC-2 (b) 370°C Interpretation of results for 300 mm/min and 500 mm/min.

5 Discussion and Conclusions

The picture-frame experiment has been successfully used to examine the intraply shearing behaviour of APC-2 at a number of temperatures within its processing range and over a range of shear rates. The suitability of a purely viscous model for modelling its behaviour under these conditions seems evident. The findings of this study are summarised in Figures 22 and 23, which show the variation of longitudinal and transverse viscosity respectively with shear rate for the models employed, and in Figures 24 and 25 which present the same information on log-log axes, giving a clearer impression of the nature of the responses recorded.

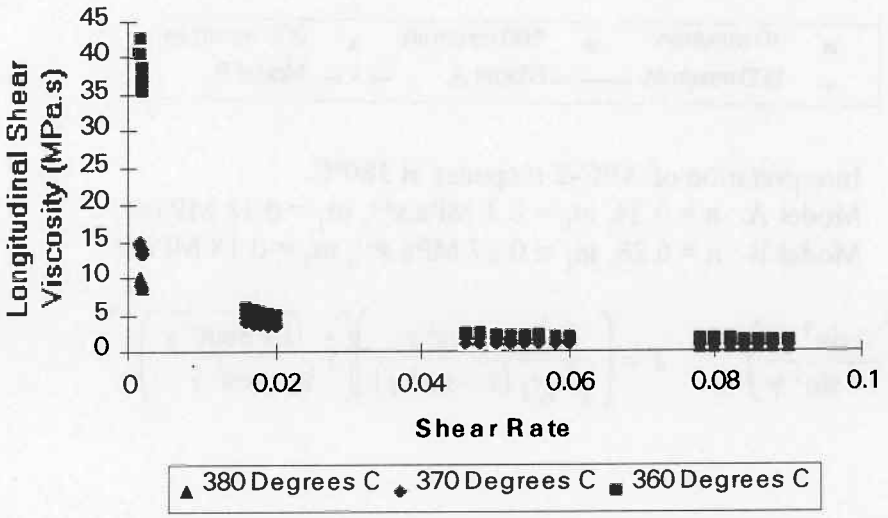

Figure 22 Variation of longitudinal shear viscosity η_L with shear rate for APC-2

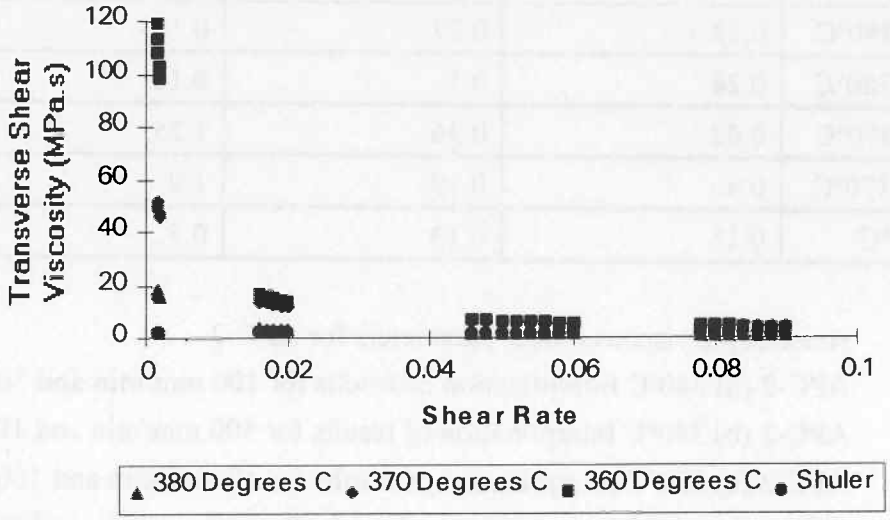

Figure 23 Variation of transverse shear viscosity η_T with shear rate for APC-2

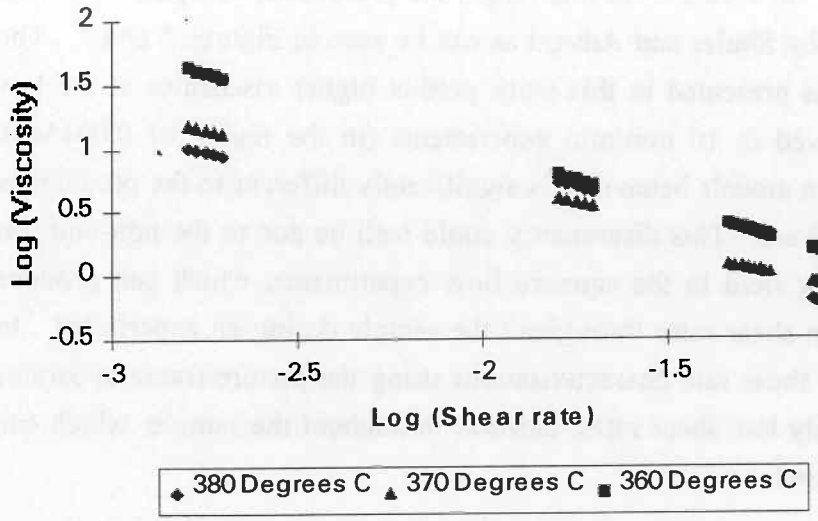

Figure 24 Log (η_L) versus Log (Shear Rate) for APC-2

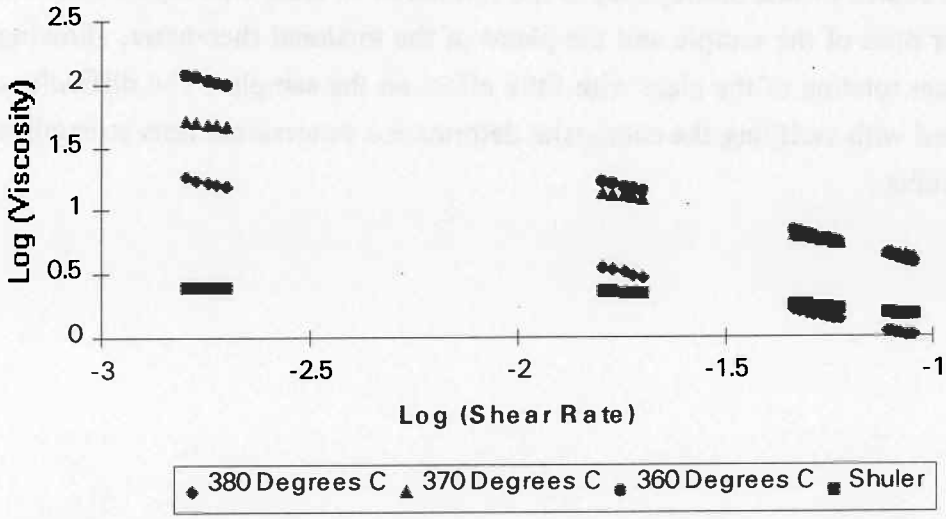

Figure 25 Log (η_T) versus Log (Shear Rate) for APC-2

Previous work on the squeeze flow of APC-2 has also produced material characterisations in terms of viscous models. Shuler and Advani present a Carreau model for transverse shear viscosity of APC-2 at 370° C which has the following form [15] :

$$\eta = \eta_0 \left[1 + \left(\lambda \dot{\gamma} \right)^2 \right]^{(n-1)/2}$$

where $n = 0.65$, $\lambda = 50.0$ and $\eta_0 = 2.5$ MPa.s.. The picture frame tests for cross-ply APC-2 laminates at 100 mm/min - 500 mm/min have involved shear rates in

the range 0.015 s^{-1} to 0.08 s^{-1}. In this range, the predictions compare very well with those given by Shuler and Advani as can be seen in Figures * and *. The power-law models presented in this work predict higher viscosities at the low shear rates involved in 10 mm/min experiments (in the region of 0.0015s^{-1}). This feature of the models behaviour is significantly different to the predictions of Shuler and Advani. This discrepancy could well be due to the non-uniform nature of the flow field in the squeeze flow experiments, which can produce large variations in shear rates throughout the sample during an experiment. In contrast, the low shear rate characterisations using the picture-frame apparatus involve exclusively low shear rates, uniform throughout the sample, which can be directly measured.

In general, the APC-2 processing temperature viscosity levels reported in this paper far exceed those obtained using torsional rheometry techniques. A possible source of this discrepancy is the formation of resin rich layers between the outer plies of the sample and the plates of the torsional rheometer, allowing significant rotation of the plate with little effect on the sample. The difficulties associated with verifying the composite deformation in torsional tests strengthen these doubts..

REFERENCES

[1] Cogswell, F.N.: *Thermoplastic Aromatic Polymer Composites,* Butterworth-Heinemann Ltd., 1992.

[2] Tucker, C.L. III, "Forming of Advanced Composites", Advanced Composites Manufacturing, edited by Gutowski, T.G., to appear.

[3] *ICI Fiberite Data Sheet 5*, Fabricating with APC-2 Composites, Fiberite Corporation (1986).

[4] Ó Brádaigh, C.M., "Sheet Forming of Composite Materials", Flow and Rheology in Polymer Composites Manufacturing, edited by S.G. Advani, Elsevier Science B.V., Amsterdam 1994.

[5] Murtagh, A.M., Monaghan, M.R., Mallon, P.J., : "Investigation of the Interply Slip Process in Continuous Fibre Thermoplastic Composites, Proceedings of the Ninth International Conference on Composite Materials (ICCM-9), Madrid, July 1993.

[6] Rogers,T.G.,"Rheological Characterisation of Anisotropic Materials", Composites, 20(1):21-27, January 1989.

[7] Spencer, A.J.M., *Deformation of Fibre-Reinforced Materials*, Clarendon Press, Oxford, 1972.

[8] Spencer, A.J.M., *Continuum Theory for Strongly Anisotropic Solids*, Springer-Verlag, New York, 1984.

[9] Groves, D.J., "A Characterisation of Shear Flow in Continuous Fibre Thermoplastic Laminates", Composites, Vol. 20, No. 1., 1989, pp28-32.

[10] Groves, D.J., Stocks, D.M., "Rheology of Thermoplastic Carbon Fibre Composites in the Elastic and Viscoelastic States", Composites Manufacturing, Vol 2 No. 3/4, 1991, pp 179-184.

[11] Groves, D.J., Bellamy, A.M., Stocks, D.M., "Anisotropic Rheology of Continuous Fibre Thermoplastic Composites", Composites, Vol. 23, No. 2, 1992, pp 75-80.

[12] Wheeler, A.B., Jones, R.S., "A Characterisation of Anisotropic Shear Flow in Continuous Fibre Composite Materials", Composites Manufacturing, Vol 2, No. 3/4, 1991.

[13] Goshawk, J.A., Jones, R.S., "The Characterisation of Continuous Fibre Reinforced Composites in Steady Shear". Proceedings of the 4th International Conference on Automated Composites, University of Nottingham, 6-7 September, 1995.

[14] Shuler, S., Advani, S.G., "Transverse Squeeze Flow of Concentrated and Aligned Fibres in Viscous Fluids", Journal of Non-Newtonian Fluid Mechanics, submitted.

[15] Wang, E.L., Gutowski, T.G., "Laps and Gaps in Thermoplastic Composites Processing", Composites Manufacturing, **2** (1991)

[16] Canavan, R.A., McGuinness, G.B., Ó Brádaigh, C.M., "Experimental Intraply Shear Testing of Glass-Fabric Reinforced Thermoplastic Melts", Proceedings of the 4th International Conference on Automated Composites, University of Nottingham, 6-7 September, 1995.

[17] McGuinness, G.B., Ó Brádaigh, C.M., *Development of Rheological Models and Picture-frame Shear Testing of Fabric Reinforced Thermoplastic Sheets,* Journal of Non-Newtonian Fluid Mechanics, submitted March 1996.

[18] Nestor, T.A., "Experimental Investigation of the Intraply Shearing Mechanism in Thermoplastic Composites Sheet-Forming", M.Eng.Sc. Thesis, Department of Mechanical Engineering, University College, Galway, 1995.

[19] *UPILEX polyimide film data sheet*, UBE Industries Ltd., 3rd Floor, 45 Conduit Street, London, W1R 9FB, U.K.

[20] Monaghan, M.R., "Mechanical Characterisation of Diaphragm Films", Ph.D. Thesis, Dept. of Mechanical Engineering, University College, Galway,1993.

[21] B.R. Duffy, *Flow of a Liquid with an Anisotropic Viscosity Tensor*, Journal of Non-Newtonian Fluid Mechanics, 4 (1978) 177-193.

[22] McGuinness, G.B., Canavan, R.A., Nestor, T.A. and Ó Brádaigh, C.M., "A Picture-Frame Intraply Shearing Test for Unidirectional and Fabric Reinforced Composite Melts", ASME Winter Annual Meeting, San Francisco, November, 1995.